International Journal of Solids and Structures 47 (2010) 25–33

Contents lists available at ScienceDirect

International Journal of Solids and Structures

journal homepage: www.elsevier.com/locate/ijsolstr

Elastic deformation of composite cylinders with cylindrically orthotropic layers

Igor Tsukrov *, Borys Drach

Department of Mechanical Engineering, University of New Hampshire, Durham, NH 03824, USA

ARTICLE INFO

Article history:
Received 13 July 2009
Received in revised form 31 August 2009
Available online 10 September 2009

Keywords:
Laminated cylinder
Composite fiber
Cylindrically orthotropic elasticity

ABSTRACT

This paper provides explicit analytical expressions for displacement and stress fields in a multilayered composite cylinder with cylindrically orthotropic layers subjected to homogeneous boundary conditions. The solutions are derived in the assumption of perfect bonding between layers. The components of displacement, strain and stress are expressed in terms of the integration constants found from boundary conditions by utilizing the transfer matrix approach. Several examples are considered. The approach is validated by comparing with previously known solutions.

1. Introduction

Elasticity solutions for layered fibers and cylindrical inclusions are of interest in several important areas of mechanics of materials including composites reinforced by fibers with imperfect or modified interface modeled as a certain interphase zone (as in Hashin, 2002), nanowires in semiconductors (see references in Shokrolahi-Zadeh and Shodja, 2008), composites with coated fibers (see, for example, Honjo, 2006), and carbon/carbon composites produced by chemical vapor infiltration (Reznik et al., 2003; Tsukrov et al., 2005). The ability to quantify deformations and stresses in interphase regions increases in importance with introduction and development of nanoreinforced materials characterized by several orders of magnitude increase in interface surface to volume ratio as compared to conventional composites.

Most of the available results dealing with interphase zones in composite materials are devoted to spherical and ellipsoidal heterogeneities, see Lutz and Zimmerman (1996, 2005), Garboczi and Bentz (1997), Wang and Jasiuk (1998), Sevostianov and Kachanov (2007), and references cited therein.

For cylindrical inclusions, i.e. fibers, the important solutions relevant to prediction of the effective elastic and thermoelastic properties can be found in Hashin and Rosen (1964), Walpole (1969), Christensen and Lo (1979), and later works of Avery and Herakovich (1986), Kanaun and Kudriavtseva (1989), Hashin (1990, 2002), Chen et al. (1990), and Hervé and Zaoui (1995). In particular, for anisotropic constituents, Avery and Herakovich (1986) derived an analytical solution for a cylindrically orthotropic fiber in an isotropic matrix subjected to thermal stresses (traction-free axisymmetric problem), and investigated the influence of fiber orthotropy on stress concentrations. Chen et al. (1990) considered thermomechanical loading of a cylindrically orthotropic fiber surrounded by transversely isotropic coating and placed in an infinite transversely isotropic matrix. For this three-phase material system, they produced solutions for the remotely applied axisymmetric, transverse shear and longitudinal shear loadings. The solutions were then used to predict the effective thermoelastic properties of the composites reinforced by coated fibers (Chen et al., 1990; Benveniste et al., 1991). In approximately the same time, Hashin (1990) analyzed a composite cylinder consisting of a fiber surrounded by a finite-thickness layer with both materials being cylindrically orthotropic. He solved the corresponding elasticity and conductivity problems utilizing homogeneous boundary conditions on the external surfaces, and produced predictions of the effective transversely isotropic elastic and conductive properties of the composite.

Recently, Honjo (2006) calculated thermal stresses and effective material parameters in the ceramic matrix composites reinforced by fibers coated with a layer of pyrolytic carbon. By considering different levels of anisotropy, he demonstrated the importance of taking into account the cylindrically-orthotropic nature of interfacial carbon coating. Shokrolahi-Zadeh and Shodja (2008) investigated elastic fields in the anisotropic layered cylinders embedded in an unbounded elastic isotropic medium. They utilized their modification of the equivalent inclusion method to produce methodology suitable for general far-field loading. Theotokoglou and Stampouloglou (2008) considered in-plane axisymmetric geometries. They produced mathematical formulation for a radially inhomogeneous cylindrically anisotropic material, and derived solutions for certain distributions of Young's modulus in the isotropic case.

Several publications have been devoted to hollow elastic tubes subjected to various boundary conditions. Gal and Dvorkin (1995) considered a plane strain problem for a cylindrically anisotropic tube subjected to the inside and outside pressure (a generalization

* Corresponding author. Tel.: +1 603 862 2086; fax: +1 603 862 1865.
E-mail address: igor.tsukrov@unh.edu (I. Tsukrov).

0020-7683/$ - see front matter © 2009 Elsevier Ltd. All rights reserved.
doi:10.1016/j.ijsolstr.2009.09.005

of the classical Lamé problem). One of their interesting observations was that, differently from the isotropic case, the anisotropic solution does not converge to any asymptotic value as the outer radius increases. Tarn and Wang (2001) provided an efficient approach to finding deformations and stresses in laminated anisotropic tubes subjected to extension, torsion, pressure, and bending. They proposed using stress components multiplied by radius as new state variables, and utilized the transfer matrix procedure to transmit the state vector to the outer surface where boundary conditions can be applied. Chatzigeorgiou et al. (2008) investigated effective elastic properties of an anisotropic hollow layered tube with discontinuous elastic coefficients and produced predictions of effective response under torsion and axisymmetric loading. Their paper also includes the most recent bibliography on mechanics of laminated (with isotropic or anisotropic layers) hollow tubes.

Only two of the above-mentioned papers deal with the situation when both the inner cylinder (fiber) and the surrounding material (matrix) are non-isotropic. However, the solutions of Hashin (1990) are limited to only one layer of a cylindrically-orthotropic material around fiber, while in Shokrolahi-Zadeh and Shodja (2008) the boundary conditions have to be applied at infinity. These deficiencies are addressed in the present paper which provides explicit expressions for stress and displacement fields in a multilayered composite cylinder with an arbitrary number of cylindrically orthotropic layers subjected to the boundary conditions assigned on the lateral surface of the outer cylinder of finite radius. The following basic homogeneous loading conditions are considered: axial tension/compression, transverse hydrostatic loading, transverse shear, and axial shear loadings. The material in each layer is modeled as linearly elastic; the strains are small. The general form of the solutions is chosen in the form presented in Hashin (1990). The layers are assumed to be perfectly bonded so that the transfer matrices approach described, for example, in Hervé and Zaoui (1995) can be utilized.

The mathematical formulation is given in Section 2. Sections 3–5 are devoted to axisymmetric problems, axial shear and transverse shear, respectively. In Section 6 several test problems are solved to illustrate the proposed solution procedure. The results are compared with the existing solutions, when available, to validate the approach.

2. Formulation of the problem

Let us consider a material system consisting of a cylindrically-orthotropic or transversely isotropic cylinder of radius R_1 surrounded by $(n-1)$ concentric layers $(R_{k-1} \leqslant r \leqslant R_k,\ k = 2, \ldots, n)$ where r, θ, z are the coordinates in the cylindrical coordinate system as shown in Fig. 1. Each layer is cylindrically orthotropic so that the stress–strain relations can be presented in the following form:

$$\begin{Bmatrix} \sigma_{rr} \\ \sigma_{\theta\theta} \\ \sigma_{zz} \\ \sigma_{\theta z} \\ \sigma_{rz} \\ \sigma_{r\theta} \end{Bmatrix} = \begin{bmatrix} C_{rr} & C_{r\theta} & C_{rz} & 0 & 0 & 0 \\ C_{r\theta} & C_{\theta\theta} & C_{\theta z} & 0 & 0 & 0 \\ C_{rz} & C_{\theta z} & C_{zz} & 0 & 0 & 0 \\ 0 & 0 & 0 & 2G_{\theta z} & 0 & 0 \\ 0 & 0 & 0 & 0 & 2G_{rz} & 0 \\ 0 & 0 & 0 & 0 & 0 & 2G_{r\theta} \end{bmatrix}^{(k)} \begin{bmatrix} \varepsilon_{rr} \\ \varepsilon_{\theta\theta} \\ \varepsilon_{zz} \\ \varepsilon_{\theta z} \\ \varepsilon_{rz} \\ \varepsilon_{r\theta} \end{bmatrix}, \tag{1}$$

where $C^{(k)}_{mn}$ and $G^{(k)}_{mn}$ are the components of the stiffness matrix of kth layer. The core cylinder $(r \leqslant R_1)$ is treated as the first layer. By choosing the external radius R_n to be much larger than R_{n-1}, we produce a model of a layered cylinder of a finite diameter (for example, a fiber surrounded by a layered interphase region) in a cylindrically orthotropic or isotropic matrix.

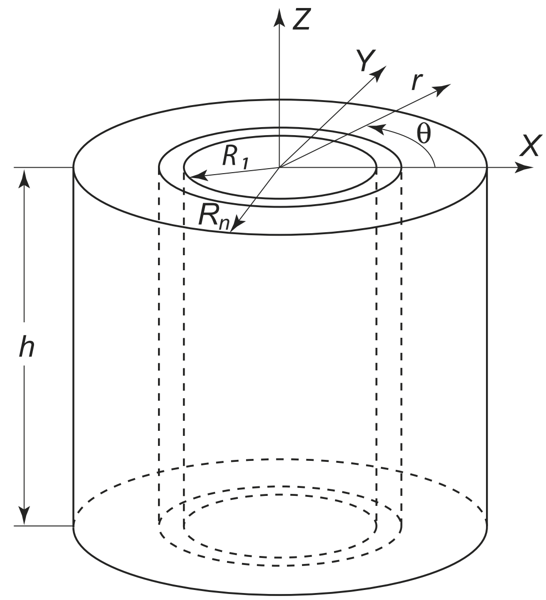

Fig. 1. Composite cylinder assemblage.

The height of the cylinder is h $(-h/2 \leqslant z \leqslant h/2)$. Some of the elastic solutions presented in this paper are derived for the infinitely long cylinder $(h \to \infty)$.

In the text to follow, parameters associated with a certain layer will be denoted by the layer number shown as a superscript or a subscript depending on the convenience of presentation. A special comment will be made when there is a possibility of confusion with other indices.

The layers are assumed to be perfectly bonded, so the displacements and radial components of traction are continuous through the interface between any two adjacent layers k and $(k+1)$:

$$\begin{aligned} & u_r^{(k)}(R_k) = u_r^{(k+1)}(R_k), \quad u_\theta^{(k)}(R_k) = u_\theta^{(k+1)}(R_k), \\ & u_z^{(k)}(R_k) = u_z^{(k+1)}(R_k), \\ & \sigma_{rr}^{(k)}(R_k) = \sigma_{rr}^{(k+1)}(R_k), \quad \sigma_{r\theta}^{(k)}(R_k) = \sigma_{r\theta}^{(k+1)}(R_k), \\ & \sigma_{rz}^{(k)}(R_k) = \sigma_{rz}^{(k+1)}(R_k). \end{aligned} \tag{2}$$

The equilibrium equations in the absence of body forces are as follows:

$$\begin{aligned} & \frac{\partial \sigma_{rr}}{\partial r} + \frac{1}{r}\frac{\partial \sigma_{r\theta}}{\partial \theta} + \frac{\partial \sigma_{rz}}{\partial z} + \frac{\sigma_{rr} - \sigma_{\theta\theta}}{r} = 0, \\ & \frac{\partial \sigma_{\theta r}}{\partial r} + \frac{1}{r}\frac{\partial \sigma_{\theta\theta}}{\partial \theta} + \frac{\partial \sigma_{\theta z}}{\partial z} + \frac{2\sigma_{\theta r}}{r} = 0, \\ & \frac{\partial \sigma_{zr}}{\partial r} + \frac{1}{r}\frac{\partial \sigma_{z\theta}}{\partial \theta} + \frac{\partial \sigma_{zz}}{\partial z} + \frac{\sigma_{zr}}{r} = 0. \end{aligned} \tag{3}$$

The relations between displacements and (small) strains are

$$\begin{aligned} & \varepsilon_{rr} = \frac{\partial u_r}{\partial r}, \quad \varepsilon_{r\theta} = \frac{1}{2}\left(\frac{\partial u_\theta}{\partial r} + \frac{1}{r}\frac{\partial u_r}{\partial \theta} - \frac{u_\theta}{r}\right), \\ & \varepsilon_{\theta\theta} = \frac{1}{r}\frac{\partial u_\theta}{\partial \theta} + \frac{u_r}{r}, \quad \varepsilon_{\theta z} = \frac{1}{2}\left(\frac{\partial u_\theta}{\partial z} + \frac{1}{r}\frac{\partial u_z}{\partial \theta}\right), \\ & \varepsilon_{zz} = \frac{\partial u_z}{\partial z}, \quad \varepsilon_{rz} = \frac{1}{2}\left(\frac{\partial u_z}{\partial r} + \frac{\partial u_r}{\partial z}\right). \end{aligned} \tag{4}$$

In the next sections, we solve the system of differential equations (1)–(4) and produce explicit expressions for stress and displacement fields in a n-layered composite cylinder with cylindrically orthotropic layers subjected to four basic loading cases: axial tension/compression, transverse hydrostatic loading, axial shear and transverse shear loadings.

3. Axial tension/compression and transverse hydrostatic loading

Consider a concentric composite cylinder subjected to the external transverse hydrostatic loading σ_T (tension or compression) and the prescribed axial elongation or contraction ε_A. The resulting deformation will be axisymmetric: there will be no angular displacement ($u_\theta = 0$), and the radial displacement will depend upon the radial coordinate only, i.e. $u_r \equiv u(r)$. Substitution of Eqs. (4) and (1) into the equilibrium equation (3) yields the following differential equation for radial displacement $u(r)$:

$$r^2u'' + ru' - \lambda^2 u + \frac{(C_{rz} - C_{\theta z})\varepsilon_A}{C_{rr}} r = 0, \tag{5}$$

where $\lambda = \sqrt{C_{\theta\theta}/C_{rr}}$, and material constants $C_{rr},\ C_{r\theta},\ C_{rz},\ C_{\theta\theta}$ assume their corresponding values for each layer. The general solution of this ordinary differential equation is given, for example, in Avery and Herakovich (1986):

$$u = A\frac{r^\lambda}{b^{\lambda-1}} + B\frac{b^{\lambda+1}}{r^\lambda} + \beta\varepsilon_A r, \tag{6}$$

where $\beta = \frac{C_{rz} - C_{\theta z}}{C_{\theta\theta} - C_{rr}}$ and A and B are integration constants.

From the general solution (6), strain–displacement relations (4) and stress–strain dependence (1) we obtain the expressions for normal stress components:

$$\begin{aligned}
\sigma_{rr} &= A(\lambda C_{rr} + C_{r\theta})\left(\frac{r}{R}\right)^{\lambda-1} + B(-\lambda C_{rr} + C_{r\theta})\left(\frac{r}{R}\right)^{-(\lambda+1)} \\
&\quad + [\beta(C_{rr} + C_{r\theta}) + C_{rz}]\varepsilon_A, \\
\sigma_{\theta\theta} &= A(\lambda C_{r\theta} + C_{\theta\theta})\left(\frac{r}{R}\right)^{\lambda-1} + B(-\lambda C_{r\theta} + C_{\theta\theta})\left(\frac{r}{R}\right)^{-(\lambda+1)} \\
&\quad + [\beta(C_{r\theta} + C_{\theta\theta}) + C_{\theta z}]\varepsilon_A, \\
\sigma_{zz} &= A(\lambda C_{rz} + C_{\theta z})\left(\frac{r}{R}\right)^{\lambda-1} + B(-\lambda C_{rz} + C_{\theta z})\left(\frac{r}{R}\right)^{-(\lambda+1)} \\
&\quad + [\beta(C_{rz} + C_{\theta z}) + C_{zz}]\varepsilon_A.
\end{aligned} \tag{7}$$

The integration constants A and B assume different values for each layer: $A_1, B_1, A_2, B_2, \ldots, A_n, B_n$. These values can be found from the continuity conditions (2). For axisymmetric deformation, we prescribe radial stresses and radial displacements to be continuous through the interface between k and $(k+1)$ layers:

$$\begin{aligned}
\sigma_{rr}^{(k)}(R_k) &= \sigma_{rr}^{(k+1)}(R_k), \\
u^{(k)}(R_k) &= u^{(k+1)}(R_k).
\end{aligned} \tag{8}$$

Following the influence matrix approach similar to that used in Hervé and Zaoui (1995) for isotropic constituents, we represent Eq. (8) in the matrix form:

$$\mathbf{J}_k(R_k)\mathbf{V}_k + \varepsilon_A\mathbf{L}_k = \mathbf{J}_{k+1}(R_k)\mathbf{V}_{k+1} + \varepsilon_A\mathbf{L}_{k+1}, \quad k = 1, \ldots, (n-1), \tag{9}$$

where $\mathbf{V}_i = [A_i, B_i]^T$ is the vector of integration constants of an ith layer ($i = 1, \ldots, n$), vector $\mathbf{L}_i$ depends on the material properties and external radius of ith layer:

$$\mathbf{L}_i = \left\{ \begin{array}{c} \beta_i R_i \\ \beta_i\left(C_{rr}^{(i)} + C_{r\theta}^{(i)}\right) + C_{rz}^{(i)} \end{array} \right\},$$

and $\mathbf{J}_i(r)$ is the following matrix:

$$\mathbf{J}_i(r) = \begin{pmatrix} \frac{r^{\lambda^{(i)}}}{R_i^{\lambda^{(i)}-1}} & \frac{R_i^{\lambda^{(i)}+1}}{r^{\lambda^{(i)}}} \\ \left(\lambda^{(i)}C_{rr}^{(i)} + C_{r\theta}^{(i)}\right)\left(\frac{r}{R_i}\right)^{\lambda^{(i)}-1} & \left(-\lambda^{(i)}C_{rr}^{(i)} + C_{r\theta}^{(i)}\right)\left(\frac{r}{R_i}\right)^{-\left(\lambda^{(i)}+1\right)} \end{pmatrix}.$$

Representation (9) allows us to construct a recurrent procedure to find all integration constants, and thus obtain the complete displacement, strain and stress fields as given by Eqs. (6), (4) and (7). The procedure is described in the text to follow.

Let us solve matrix equation (9) for the set of integration constants of the $(k+1)$th layer:

$$\mathbf{V}_{k+1} = \mathbf{N}^{(k+1)}\mathbf{V}_k + \varepsilon_A\mathbf{M}^{(k+1)}, \tag{10}$$

where

$$\mathbf{N}^{(k+1)} = \mathbf{J}_{k+1}^{-1}(R_k)\cdot\mathbf{J}_k(R_k), \quad \mathbf{M}^{(k+1)} = \mathbf{J}_{k+1}^{-1}(R_k)[\mathbf{L}_k(R_k) - \mathbf{L}_{k+1}(R_k)].$$

The explicit expression for matrix $\mathbf{N}^{(k+1)}$ is

$$\mathbf{N}^{(k+1)} = -\frac{R_k}{2\lambda^{(k+1)}C_{rr}^{(k+1)}R_{k+1}^2}\begin{pmatrix} N_{11}^{(k+1)} & N_{12}^{(k+1)} \\ N_{21}^{(k+1)} & N_{22}^{(k+1)} \end{pmatrix},$$

where

$$\begin{aligned}
N_{11}^{(k+1)} &= \left(C_{r\theta}^{(k+1)} - \lambda^{(k+1)}C_{rr}^{(k+1)} - \lambda^{(k)}C_{rr}^{(k)} - C_{r\theta}^{(k)}\right)\frac{R_{k+1}^{\lambda^{(k+1)}+1}}{R_k^{\lambda^{(k)}}}, \\
N_{12}^{(k+1)} &= \left(C_{r\theta}^{(k+1)} - \lambda^{(k+1)}C_{rr}^{(k+1)} + \lambda^{(k)}C_{rr}^{(k)} - C_{r\theta}^{(k)}\right)\frac{R_{k+1}^{\lambda^{(k+1)}+1}}{R_k^{\lambda^{(k)}}}, \\
N_{21}^{(k+1)} &= \left(-C_{r\theta}^{(k+1)} - \lambda^{(k+1)}C_{rr}^{(k+1)} + \lambda^{(k)}C_{rr}^{(k)} + C_{r\theta}^{(k)}\right)\frac{R_k^{\lambda^{(k+1)}}}{R_{k+1}^{\lambda^{(k+1)}-1}}, \\
N_{22}^{(k+1)} &= \left(-C_{r\theta}^{(k+1)} - \lambda^{(k+1)}C_{rr}^{(k+1)} - \lambda^{(k)}C_{rr}^{(k)} + C_{r\theta}^{(k)}\right)\frac{R_k^{\lambda^{(k+1)}}}{R_{k+1}^{\lambda^{(k+1)}-1}}.
\end{aligned}$$

Matrix $\mathbf{M}^{(k+1)}$ is given by:

$$\mathbf{M}^{(k+1)} = \frac{1}{2\lambda^{(k+1)}C_{rr}^{(k+1)}}\left\{ \begin{array}{c} M_1^{(k+1)} \\ M_2^{(k+1)} \end{array} \right\},$$

where

$$\begin{aligned}
M_1^{(k+1)} &= \left(\frac{R_{k+1}}{R_k}\right)^{\lambda^{(k+1)}-1}\left[\beta_k\left(C_{rr}^{(k)} + C_{r\theta}^{(k)}\right) + C_{rz}^{(k)} - \beta_{k+1}\left(C_{rr}^{(k+1)} + C_{r\theta}^{(k+1)}\right)\right. \\
&\quad \left. - C_{rz}^{(k+1)} + \left(\lambda^{(k+1)}C_{rr}^{(k+1)} - C_{r\theta}^{(k+1)}\right)(\beta_k - \beta_{k+1})\right], \\
M_2^{(k+1)} &= -\left(\frac{R_k}{R_{k+1}}\right)^{\lambda^{(k+1)}+1}\left[\beta_k\left(C_{rr}^{(k)} + C_{r\theta}^{(k)}\right) + C_{rz}^{(k)} - \beta_{k+1}\left(C_{rr}^{(k+1)} + C_{r\theta}^{(k+1)}\right)\right. \\
&\quad \left. - C_{rz}^{(k+1)} + \left(\lambda^{(k+1)}C_{rr}^{(k+1)} + C_{r\theta}^{(k+1)}\right)(\beta_k - \beta_{k+1})\right].
\end{aligned}$$

Formula (10) can be utilized to express the integration constants in any $(k+1)$th layer in terms of integration constants of the 1st layer (inner core cylinder):

$$\mathbf{V}_{k+1} = \mathbf{Q}^{(k+1)}\mathbf{V}_1 + \varepsilon_A\mathbf{P}^{(k+1)}, \tag{11}$$

where

$$\mathbf{Q}^{(k+1)} = \prod_{j=k+1}^{2}\mathbf{N}^{(j)}, \quad \mathbf{P}^{(k+1)} = \left\{ \begin{array}{c} P_1^{(k+1)} \\ P_2^{(k+1)} \end{array} \right\},$$

and the components of $\mathbf{P}^{(k+1)}$ are as follows:

$$P_1^{(k+1)} = \frac{1}{2\lambda^{(k+1)}C_{rr}^{(k+1)}}\left(\frac{R_{k+1}}{R_k}\right)^{\lambda^{(k+1)}-1}\left[\beta_k\left(C_{rr}^{(k)}+C_{r\theta}^{(k)}\right)\right.$$
$$+C_{rz}^{(k)}-\beta_{k+1}\left(C_{rr}^{(k+1)}+C_{r\theta}^{(k+1)}\right)-C_{rz}^{(k+1)}+\left(\lambda^{(k+1)}C_{rr}^{(k+1)}-C_{r\theta}^{(k+1)}\right)$$
$$\left.\times\left(\beta_k-\beta_{k+1}\right)\right]+\sum_{i=1}^{k-1}\frac{1}{2\lambda^{(i+1)}C_{rr}^{(i+1)}}\left(\frac{R_{i+1}}{R_i}\right)^{\lambda^{(i+1)}-1}\left[\beta_i\left(C_{rr}^{(i)}+C_{r\theta}^{(i)}\right)\right.$$
$$+C_{rz}^{(i)}-\beta_{i+1}\left(C_{rr}^{(i+1)}+C_{r\theta}^{(i+1)}\right)-C_{rz}^{(i+1)}+\left(\lambda^{(i+1)}C_{rr}^{(i+1)}-C_{r\theta}^{(i+1)}\right)$$
$$\left.\times\left(\beta_i-\beta_{i+1}\right)\right]\left(\prod_{j=k+1}^{i+2}\mathbf{N}^{(j)}\right),$$

$$P_2^{(k+1)} = -\frac{1}{2\lambda^{(k+1)}C_{rr}^{(k+1)}}\left(\frac{R_k}{R_{k+1}}\right)^{\lambda^{(k+1)}+1}\left[\beta_k\left(C_{rr}^{(k)}+C_{r\theta}^{(k)}\right)\right.$$
$$+C_{rz}^{(k)}-\beta_{k+1}\left(C_{rr}^{(k+1)}+C_{r\theta}^{(k+1)}\right)-C_{rz}^{(k+1)}+\left(\lambda^{(k+1)}C_{rr}^{(k+1)}+C_{r\theta}^{(k+1)}\right)$$
$$\left.\times\left(\beta_k-\beta_{k+1}\right)\right]-\sum_{i=1}^{k-1}\frac{1}{2\lambda^{(i+1)}C_{rr}^{(i+1)}}\left(\frac{R_i}{R_{i+1}}\right)^{\lambda^{(i+1)}+1}\left[\beta_i\left(C_{rr}^{(i)}+C_{r\theta}^{(i)}\right)\right.$$
$$+C_{rz}^{(i)}-\beta_{i+1}\left(C_{rr}^{(i+1)}+C_{r\theta}^{(i+1)}\right)-C_{rz}^{(i+1)}+\left(\lambda^{(i+1)}C_{rr}^{(i+1)}+C_{r\theta}^{(i+1)}\right)$$
$$\left.\times\left(\beta_i-\beta_{i+1}\right)\right]\left(\prod_{j=k+1}^{i+2}\mathbf{N}^{(j)}\right).$$

In the formulae above, multiplication of the matrices is performed in the prescribed order so that, for example:

$$\prod_{j=4}^{2}\mathbf{N}^{(j)} = \mathbf{N}_4\mathbf{N}_3\mathbf{N}_2.$$

Expanding formula (11) and assigning $B_1 = 0$ for the core cylinder to avoid singularity of the radial displacement at the center ($r = 0$), we produce the following representation for the vector of integration constants:

$$\begin{Bmatrix} A_{k+1} \\ B_{k+1} \end{Bmatrix} = \begin{bmatrix} Q_{11}^{(k+1)} & Q_{12}^{(k+1)} \\ Q_{21}^{(k+1)} & Q_{22}^{(k+1)} \end{bmatrix}\begin{Bmatrix} A_1 \\ 0 \end{Bmatrix} + \varepsilon_A\begin{Bmatrix} P_1^{(k+1)} \\ P_2^{(k+1)} \end{Bmatrix}, \quad k = 1,\ldots,(n-1). \tag{12}$$

Thus, integration constants of any layer can be expressed in terms of the constant A_1. In particular, for the outer, nth, layer:

$$A_n = Q_{11}^{(n)}A_1 + \varepsilon_A P_1^{(n)},$$
$$B_n = Q_{21}^{(n)}A_1 + \varepsilon_A P_2^{(n)}.$$

Alternatively, all integration constants can be expressed in terms of A_n. First, we express A_1 as

$$A_1 = \frac{1}{Q_{11}^{(n)}}\left(A_n - \varepsilon_A P_1^{(n)}\right). \tag{13}$$

Then, for each ith layer:

$$\begin{aligned} A_i &= \tfrac{Q_{11}^{(i)}}{Q_{11}^{(n)}}A_n + \varepsilon_A\left(P_1^{(i)} - \tfrac{Q_{11}^{(i)}}{Q_{11}^{(n)}}P_1^{(n)}\right), \\ B_i &= \tfrac{Q_{21}^{(i)}}{Q_{11}^{(n)}}A_n + \varepsilon_A\left(P_2^{(i)} - \tfrac{Q_{21}^{(i)}}{Q_{11}^{(n)}}P_1^{(n)}\right), \end{aligned} \quad i = 1,2,\ldots,n. \tag{14}$$

Using these expressions for the integration constants, displacements and stresses in each layer can be found from formulae (6) and (7) if parameters ε_A and A_n are known. To determine ε_A and A_n, the boundary conditions of the corresponding problem are utilized as presented below.

3.1. Longitudinal deformation of the cylinder

In the case of longitudinal elongation or contraction of the cylinder ($\varepsilon_z = \varepsilon_A$) with no lateral constraints, the boundary conditions are

$$u_z = \varepsilon_A z, \quad \sigma_{rr}(R_n) = 0. \tag{15}$$

Substituting $r = R_n$ in the expression for the radial component of stress (7), the following equation is obtained:

$$A_n\left(\lambda^{(n)}C_{rr}^{(n)} + C_{r\theta}^{(n)}\right) + B_n\left(-\lambda^{(n)}C_{rr}^{(n)} + C_{r\theta}^{(n)}\right) + \left[\beta^{(n)}\left(C_{rr}^{(n)} + C_{r\theta}^{(n)}\right) + C_{rz}^{(n)}\right]\varepsilon_A = 0.$$

This equation contains two integration constants of the nth layer A_n and B_n. Expressing B_n in terms of A_n and ε_A by means of the second equation in (14), we derive the expression for the integration constant A_n:

$$A_n = -\frac{\varepsilon_A\left\{\left(P_2^{(n)} - \frac{Q_{21}^{(n)}}{Q_{11}^{(n)}}P_1^{(n)}\right)\left(-\lambda^{(n)}C_{rr}^{(n)} + C_{r\theta}^{(n)}\right) + \left[\beta^{(n)}\left(C_{rr}^{(n)} + C_{r\theta}^{(n)}\right) + C_{rz}^{(n)}\right]\right\}}{\left(\lambda^{(n)}C_{rr}^{(n)} + C_{r\theta}^{(n)}\right) + \frac{Q_{21}^{(n)}}{Q_{11}^{(n)}}\left(-\lambda^{(n)}C_{rr}^{(n)} + C_{r\theta}^{(n)}\right)}. \tag{16}$$

Representation (16) and formulae (14) can then be utilized to calculate the integration constants for all layers.

3.2. Transverse hydrostatic loading

For uniform external lateral compression or tension of the cylinder, the boundary conditions are

$$u_z(z = \pm h/2) = 0, \quad \sigma_{rr}(R_n) = \sigma_T. \tag{17}$$

The first condition of (17) defines the plane strain mode of deformation so that $\varepsilon_A = 0$. The second condition can be utilized to produce the equation for the integration constants A_n and B_n. Substituting the expanded expression from (7) for $r = R_n$, we obtain:

$$A_n\left(\lambda^{(n)}C_{rr}^{(n)} + C_{r\theta}^{(n)}\right) + B_n\left(-\lambda^{(n)}C_{rr}^{(n)} + C_{r\theta}^{(n)}\right) = \sigma_T.$$

Expressing B_n in terms of A_n, see (14), we produce the desired formula for the integration constant A_n:

$$A_n = \frac{\sigma_T}{\left(\lambda^{(n)}C_{rr}^{(n)} + C_{r\theta}^{(n)}\right) + \frac{Q_{21}^{(n)}}{Q_{11}^{(n)}}\left(-\lambda^{(n)}C_{rr}^{(n)} + C_{r\theta}^{(n)}\right)}, \tag{18}$$

which, in combination with (14), can be used to calculate A_i and B_i ($i = 1,2,\ldots,n$), and thus the complete expressions for displacement, strain and stress fields in the cylinder (see formulae (6), (4) and (7)).

4. Axial shear deformation

We assume that the cylinder is subjected to the longitudinal shear $\varepsilon_{yz} = s$ such that the in-plane displacements of the cylinder are

$$u_r = sz\cos\theta, \quad u_\theta = -sz\sin\theta, \tag{19}$$

and the axial displacement of the lateral surface is given by

$$u_z = sR_n\cos\theta. \tag{20}$$

The ends $z = \pm h/2$ of the cylinder are traction-free. To determine the distribution of vertical displacements through the cross-sectional area of the multilayered cylinder, we generalize the solution used in Hashin (1990). Displacement u_z is represented in the form

$$u_z = s\psi(r,\theta), \tag{21}$$

where ψ is an unknown function. Calculating the stresses by substituting the expressions for displacements into formulae (4) and (1) we observe that there are two non-zero components

$$\begin{aligned} \sigma_{rz} &= sG_{rz}\left[\frac{\partial\psi}{\partial r} + \cos\theta\right], \\ \sigma_{\theta z} &= sG_{\theta z}\left[\frac{\partial\psi}{r\partial\theta} - \sin\theta\right], \end{aligned} \tag{22}$$

Substitution of these stresses into the third equilibrium equation of (3) yields the following second-order differential equation for unknown function $\psi(r,\theta)$:

$$G_{rz}\left[\frac{\partial^2\psi}{\partial r^2} + \frac{\partial\psi}{r\partial r}\right] + G_{\theta z}\frac{\partial^2\psi}{r^2\partial\theta^2} + \frac{G_{rz} - G_{\theta z}}{r} = 0. \tag{23}$$

It can be observed that representation

$$\psi(r,\theta) = \left(Ar^{\lambda} + Br^{-\lambda} - r\right)\cos\theta, \tag{24}$$

satisfies Eq. (23), where $\lambda = \sqrt{G_{\theta z}/G_{rz}}$ and A, B are the integration constants that are different for each layer. To find these constants we make use of continuity conditions (2).

The requirements of continuous displacements $u_z^{(k)}(R_k) = u_z^{(k+1)}(R_k)$ and tractions $\sigma_{rz}^{(k)}(R_k) = \sigma_{rz}^{(k+1)}(R_k)$ on the interface between kth and $(k+1)$th layers, produce the following equations relating their constants:

$$\begin{cases} A_kR_k^{\lambda_k} + B_kR_k^{-\lambda_k} = A_{k+1}R_k^{\lambda_{k+1}} + B_{k+1}R_k^{-\lambda_{k+1}}, \\ G_{rz}^{k}\left(\lambda_kA_kR_k^{\lambda_k-1} - \lambda_kB_kR_k^{-\lambda_k-1}\right) = G_{rz}^{k+1}\left(\lambda_{k+1}A_{k+1}R_k^{\lambda_{k+1}-1} - \lambda_{k+1}B_{k+1}R_k^{-\lambda_{k+1}-1}\right). \end{cases}$$

In the matrix form these equations can be written as

$$\mathbf{J}_k(R_k)\mathbf{V}_k + \mathbf{L}_k(R_k) = \mathbf{J}_{k+1}(R_k)\mathbf{V}_{k+1} + \mathbf{L}_{k+1}(R_k), \tag{25}$$

where $\mathbf{V}_i = [A_i, B_i]^T$ is the vector of integration constants of the ith layer, and $\mathbf{L}_i(r)$ and $\mathbf{J}_i(r)$ are the coefficient matrices:

$$\mathbf{L}_i(r) = \begin{Bmatrix} -r \\ 0 \end{Bmatrix}, \quad \mathbf{J}_i(r) = \begin{pmatrix} r^{\lambda_i} & r^{-\lambda_i} \\ \lambda_iG_{rz}^{(i)}r^{\lambda_i-1} & -\lambda_iG_{rz}^{(i)}r^{-\lambda_i-1} \end{pmatrix}, \qquad i = 1,2,\ldots,n.$$

Eq. (25) can be used to express the integration constants for any $(k+1)$th layer in terms of the inner core integration constants A_1, B_1:

$$\mathbf{V}_{k+1} = \mathbf{Q}^{(k+1)}\mathbf{V}_1, \tag{26}$$

where $\mathbf{Q}^{(k+1)} = \prod_{j=k+1}^{2}\mathbf{N}^{(j)}$, and

$$\mathbf{N}^{(i)} = -\frac{R_{i-1}}{2\lambda^{(i)}G_{rz}^{(i)}}\begin{pmatrix} N_{11}^{(i)} & N_{12}^{(i)} \\ N_{21}^{(i)} & N_{22}^{(i)} \end{pmatrix},$$

with the components

$$\begin{aligned} N_{11}^{(i)} &= -R_{i-1}^{\lambda^{(i-1)}-\lambda^{(i)}-1}\left(\lambda^{(i-1)}G_{rz}^{(i-1)} + \lambda^{(i)}G_{rz}^{(i)}\right), \\ N_{12}^{(i)} &= R_{i-1}^{-\lambda^{(i-1)}-\lambda^{(i)}-1}\left(\lambda^{(i-1)}G_{rz}^{(i-1)} - \lambda^{(i)}G_{rz}^{(i)}\right), \\ N_{21}^{(i)} &= R_{i-1}^{\lambda^{(i-1)}+\lambda^{(i)}-1}\left(\lambda^{(i-1)}G_{rz}^{(i-1)} - \lambda^{(i)}G_{rz}^{(i)}\right), \\ N_{22}^{(i)} &= -R_{i-1}^{-\lambda^{(i-1)}+\lambda^{(i)}-1}\left(\lambda^{(i-1)}G_{rz}^{(i-1)} + \lambda^{(i)}G_{rz}^{(i)}\right). \end{aligned}$$

However, the integration constant B_1 should be chosen to be zero to avoid singularity of the stresses at the axis of the cylinder $(r = 0)$, see Eqs. (22) and (24). Thus, the integration constants of the ith layer are given by

$$A_i = Q_{11}^{(i)}A_1, \quad B_i = Q_{21}^{(i)}A_1. \tag{27}$$

Note, that formulae (26) and (27) can be used to relate A_n and B_n as follows:

$$B_n = \frac{Q_{21}^{(n)}}{Q_{11}^{(n)}}A_n. \tag{28}$$

To determine the remaining independent integration constant, we utilize boundary equation (20). Substituting expressions (21) and (24) we obtain:

$$A_nR_n^{\lambda^{(n)}} + B_nR_n^{-\lambda^{(n)}} = 2R_n,$$

which can be solved in combination with (28) to produce:

$$A_n = \frac{2}{R_n^{\lambda^{(n)}-1} + \frac{Q_{21}^{(n)}}{Q_{11}^{(n)}}R_n^{-\lambda^{(n)}-1}}.$$

Now, from (27),

$$A_1 = \frac{A_n}{Q_{11}^{(n)}}, \tag{29}$$

and all integration constants can be readily obtained.

5. Transverse shear

In this plane strain problem, we are looking for displacements in the following form:

$$\begin{aligned} u_r &= u(r)\sin 2\theta, \\ u_\theta &= v(r)\cos 2\theta, \end{aligned} \tag{30}$$

where $u(r)$ and $v(r)$ are two unknown functions of radius r. Substituting these displacements into (4) we obtain strains as

$$\begin{aligned} \varepsilon_{rr} &= u'\sin 2\theta, \\ \varepsilon_{\theta\theta} &= \frac{(u-2v)}{r}\sin 2\theta, \\ \gamma_{r\theta} &= \left(\frac{(2u-v)}{r} + v'\right)\cos 2\theta, \end{aligned} \tag{31}$$

which results in the following representation for stresses:

$$\begin{aligned} \sigma_{rr} &= \left(C_{rr}u' + C_{r\theta}\frac{(u-2v)}{r}\right)\sin 2\theta, \\ \sigma_{\theta\theta} &= \left(C_{r\theta}u' + C_{\theta\theta}\frac{(u-2v)}{r}\right)\sin 2\theta, \\ \tau_{r\theta} &= G_{r\theta}\left(\frac{2u-v}{r} + v'\right)\cos 2\theta. \end{aligned} \tag{32}$$

The equilibrium equation (3) can then be rewritten as a system of two homogeneous differential equations of the second order:

$$\begin{cases} C_{rr}(r^2u'' + ru') - (C_{\theta\theta} + 4G_{r\theta})u - 2(C_{r\theta} + G_{r\theta})rv' + 2(C_{\theta\theta} + G_{r\theta})v = 0, \\ 2(C_{r\theta} + G_{r\theta})ru' + 2(C_{\theta\theta} + G_{r\theta})u + G_{r\theta}(r^2v'' + rv') - (4C_{\theta\theta} + G_{r\theta})v = 0. \end{cases} \tag{33}$$

Solution of this system is sought in the following form:

$$u(r) = Ar^{\alpha}, \quad v(r) = Br^{\alpha},$$

where A and B are some integration constants. The requirement of existence of non-zero solution yields the following characteristic equation for values of α:

$$D\alpha^4 + F\alpha^2 + H = 0, \tag{34}$$

where

$$D = C_{rr}G_{r\theta},$$
$$F = 4(C_{r\theta}+G_{r\theta})^2 - C_{rr}(4C_{\theta\theta}+G_{r\theta}) - G_{r\theta}(C_{\theta\theta}+4G_{r\theta}),$$
$$H = 9G_{r\theta}C_{\theta\theta}.$$

The roots of Eq. (34) depend on the material properties of the considered layer. For all materials encountered by the authors so far, these roots have been real numbers. Similar observation is reported in Hashin (1990). In particular, in the case of the isotropic material with Young's modulus E and Poisson's ratio ν, the discriminant of the bi-quadratic equation (34) is positive and equal to $16E^4(1-\nu)^2/[(1+\nu)^4(1-2\nu)^2]$. The roots then are $\alpha_{1,2}=\pm 1$, $\alpha_{3,4}=\pm 3$ which is consistent with the form of the solution presented in Savin (1961) and Christensen and Lo (1979). In a more general case, for any real roots $\alpha_1,\alpha_2,\alpha_3,\alpha_4$ the representations for $u(r)$ and $v(r)$ are

$$u(r) = A_1r^{\alpha_1}+A_2r^{\alpha_2}+A_3r^{\alpha_3}+A_4r^{\alpha_4},$$
$$v(r) = B_1r^{\alpha_1}+B_2r^{\alpha_2}+B_3r^{\alpha_3}+B_4r^{\alpha_4}. \tag{35}$$

Integration constants A_i and B_i $(i=1,\ldots,4)$ are linearly dependent. Utilizing, for example, the first equation of (33), we obtain:

$$B_i = g_iA_i, \quad (i=1,\ldots,4),$$

where

$$g_i = \frac{\alpha_i^2C_{rr} - (C_{\theta\theta}+4G_{r\theta})}{2(C_{r\theta}+G_{r\theta})\alpha_i - 2(C_{\theta\theta}+G_{r\theta})}.$$

Thus, all components of displacement and stress for each kth layer can be expressed in terms of parameters α_i, g_i, A_i $(i=1,\ldots,4)$ which are different for different layers:

$$u_r = \sum_{i=1}^{4} A_ir^{\alpha_i}\sin 2\theta, \quad u_\theta = \sum_{i=1}^{4} g_iA_ir^{\alpha_i}\cos 2\theta,$$
$$\sigma_{rr} = \sum_{i=1}^{4}\left[(A_ir^{\alpha_i-1})(C_{rr}\alpha_i + C_{r\theta}(1-2g_i))\right]\sin 2\theta,$$
$$\sigma_{\theta\theta} = \sum_{i=1}^{4}\left[(A_ir^{\alpha_i-1})(C_{r\theta}\alpha_i + C_{\theta\theta}(1-2g_i))\right]\sin 2\theta,$$
$$\sigma_{r\theta} = G_{r\theta}\sum_{i=1}^{4}\left[(A_ir^{\alpha_i-1})(2+(\alpha_i-1)g_i)\right]\cos 2\theta. \tag{36}$$

Parameters α_1–α_4, g_1–g_4 are expressed in terms of material moduli, while integration constants A_1–A_4 for each layer are found from the continuity and boundary conditions as follows.

We start by utilizing the continuity conditions between two adjacent layers, k and $(k+1)$. Substituting the expressions for stresses (36) into (2) we obtain the following matrix equation relating vectors of the integration constants:

$$\mathbf{J}_k(R_k)\mathbf{V}_k = \mathbf{J}_{k+1}(R_k)\mathbf{V}_{k+1}, \tag{37}$$

where $\mathbf{V}_i = \left[A_1^{(i)} \quad A_2^{(i)} \quad A_3^{(i)} \quad A_4^{(i)}\right]^T$ is the vector of integration constants of ith layer. Matrix $\mathbf{J}_i(r)$ is given by

$$\mathbf{J}_i(r) = \begin{pmatrix} r^{\alpha_1^{(i)}}\sin 2\theta & r^{\alpha_2^{(i)}}\sin 2\theta & r^{\alpha_3^{(i)}}\sin 2\theta & r^{\alpha_4^{(i)}}\sin 2\theta \\ g_1^{(i)}r^{\alpha_1^{(i)}}\cos 2\theta & g_2^{(i)}r^{\alpha_2^{(i)}}\cos 2\theta & g_3^{(i)}r^{\alpha_3^{(i)}}\cos 2\theta & g_4^{(i)}r^{\alpha_4^{(i)}}\cos 2\theta \\ p_1^{(i)}r^{\alpha_1^{(i)}-1}\sin 2\theta & p_2^{(i)}r^{\alpha_2^{(i)}-1}\sin 2\theta & p_3^{(i)}r^{\alpha_3^{(i)}-1}\sin 2\theta & p_4^{(i)}r^{\alpha_4^{(i)}-1}\sin 2\theta \\ q_1^{(i)}r^{\alpha_1^{(i)}-1}\cos 2\theta & q_2^{(i)}r^{\alpha_2^{(i)}-1}\cos 2\theta & q_3^{(i)}r^{\alpha_3^{(i)}-1}\cos 2\theta & q_4^{(i)}r^{\alpha_4^{(i)}-1}\cos 2\theta \end{pmatrix},$$

where $p_j^{(i)} = C_{rr}^{(i)}\alpha_j^{(i)} + C_{r\theta}^{(i)}\left(1-2g_j^{(i)}\right)$, $q_j^{(i)} = G_{r\theta}^{(i)}\left[2+\left(\alpha_j^{(i)}-1\right)g_j^{(i)}\right]$.

From Eq. (37) all integration constants can be expressed in terms of the set of constants for one layer, for example, the inner core $A_1^{(1)}$–$A_4^{(1)}$.

$$\mathbf{V}_{k+1} = \mathbf{Q}^{(k+1)}\mathbf{V}_1, \tag{38}$$

where, similarly to (11), $\mathbf{Q}^{(k+1)} = \prod_{j=k+1}^{2}\left[\mathbf{J}_j^{-1}(R_{j-1})\mathbf{J}_{j-1}(R_{j-1})\right]$.

Let us find the integration constants for a composite cylinder subjected to the homogeneous boundary conditions at infinity $(r\to\infty)$:

$$u_r = sr\sin 2\theta, \quad u_\theta = sr\cos 2\theta, \tag{39}$$

which yield the following expressions for stresses in the exterior layer:

$$\sigma_{rr} = s\left(C_{rr}^{(n)} - C_{r\theta}^{(n)}\right), \quad \sigma_{\theta\theta} = s\left(C_{r\theta}^{(n)} - C_{\theta\theta}^{(n)}\right), \quad \sigma_{r\theta} = 2sG_{r\theta}^{(n)}. \tag{40}$$

We assume that the exterior layer is isotropic. The roots of characteristic equations in this case are

$$\alpha_{1,2}^{(n)} = \pm 1, \quad \alpha_{3,4}^{(n)} = \pm 3,$$

and the displacements are given by the following formulae:

$$u^{(n)} = A_1^{(n)}r + \frac{A_2^{(n)}}{r} + A_3^{(n)}r^3 + \frac{A_4^{(n)}}{r^3},$$
$$v^{(n)} = g_1^{(n)}A_1^{(n)}r + \frac{g_2^{(n)}A_2^{(n)}}{r} + g_3^{(n)}A_3^{(n)}r^3 + \frac{g_4^{(n)}A_4^{(n)}}{r^3}. \tag{41}$$

Substituting these expressions into the boundary conditions (40) we obtain $A_1^{(n)} = s$, $A_3^{(n)} = 0$. The remaining $A_2^{(n)}$ and $A_4^{(n)}$ can be found from (38):

$$A_2^{(n)} = Q_{21}^{(n)}A_1^{(1)} + Q_{22}^{(n)}A_2^{(1)} + Q_{23}^{(n)}A_3^{(1)} + Q_{24}^{(n)}A_4^{(1)},$$
$$A_4^{(n)} = Q_{41}^{(n)}A_1^{(1)} + Q_{42}^{(n)}A_2^{(1)} + Q_{43}^{(n)}A_3^{(1)} + Q_{44}^{(n)}A_4^{(1)}, \tag{42}$$

where $A_2^{(1)}$ and $A_4^{(1)}$ are set to be zero to avoid singularity at the center of the composite cylinder. We consider the first and the third equations of the system (38) to find $A_1^{(1)}$ and $A_3^{(1)}$:

$$\begin{cases} s = Q_{11}^{(n)}A_1^{(1)} + Q_{13}^{(n)}A_3^{(1)}, \\ 0 = Q_{31}^{(n)}A_1^{(1)} + Q_{33}^{(n)}A_3^{(1)}, \end{cases}$$

which yields $A_1^{(1)} = \frac{sQ_{33}^{(n)}}{Q_{11}^{(n)}Q_{33}^{(n)} - Q_{13}^{(n)}Q_{31}^{(n)}}$ and $A_3^{(1)} = -\frac{Q_{31}^{(n)}A_1^{(1)}}{Q_{33}^{(n)}}$. All integration constants in the solution (36) are thus found.

6. Examples and validation

Several test problems are solved to illustrate the developed analytical procedure and validate it against the existing solutions. In particular, we consider the canonical 2D case of a circular isotropic inhomogeneity in an infinite plane under remotely applied homogeneous loading. Then, we derive the solution for a fiber surrounded by anisotropic interphase zone and loaded as described in Shokrolahi-Zadeh and Shodja (2008) and compare our predictions with their results. And, finally, we provide solutions for hydrostatic loading of a carbon fiber coated by several layers of cylindrically orthotropic pyrolytic carbon.

6.1. Hydrostatic loading and transverse shear in r, θ-plane

Consider plane strain problem for an isotropic elastic inclusion with Young's modulus E_1, Poisson's ratio ν_1 and radius $R_1 = a$ surrounded by a concentric layer of isotropic elastic material of radius $R_2 = R$ with material properties E_2 and. ν_2. The solution of this problem in the case of an infinitely large outside layer $(R\to\infty)$ can be found in Muskhelishvili (1953), see also Kachanov et al. (2003) for convenient formulae. Muskhelishvili's solution is provided for unidirectional in-plane tension only, however, the hydrostatic and pure in-plane shear cases can be obtained by superposition.

Table 1
Mechanical properties of constituents in composite cylinder assemblage.

	E_r	E_θ	E_z	$\nu_{r\theta}$	$\nu_{\theta z}$	ν_{rz}	$G_{r\theta}$	$G_{\theta z}$	G_{rz}
Core	5	5	10	0.4	0.3	0.3	25/14	2	2
Matrix	1	1	1	0.3	0.3	0.3	5/13	5/13	5/13
Shell 1	3	3	3	0.2	0.2	0.2	5/4	5/4	5/4
Shell 2	6	3	3	0.3	0.2	0.3	1	5/4	1
Shell 3	12	3	3	0.4	0.2	0.4	3/4	5/4	3/4

For illustration purposes, let us choose the following values of the material parameters: $E_1 = 10$; $E_2 = 1$; $\nu_1 = 0.2$; $\nu_2 = 0.4$. The stiffness matrices are then

$$\mathbf{C}^{(1)} = \begin{pmatrix} 1.11 & 2.78 & 2.78 & 0 & 0 & 0 \\ 2.78 & 1.11 & 2.78 & 0 & 0 & 0 \\ 2.78 & 2.78 & 1.11 & 0 & 0 & 0 \\ 0 & 0 & 0 & 4.17 & 0 & 0 \\ 0 & 0 & 0 & 0 & 4.17 & 0 \\ 0 & 0 & 0 & 0 & 0 & 4.17 \end{pmatrix},$$

$$\mathbf{C}^{(2)} = \begin{pmatrix} 2.14 & 1.43 & 1.43 & 0 & 0 & 0 \\ 1.43 & 2.14 & 1.43 & 0 & 0 & 0 \\ 1.43 & 1.43 & 2.14 & 0 & 0 & 0 \\ 0 & 0 & 0 & 0.36 & 0 & 0 \\ 0 & 0 & 0 & 0 & 0.36 & 0 \\ 0 & 0 & 0 & 0 & 0 & 0.36 \end{pmatrix}.$$

In the case of *transverse hydrostatic loading*, the solution is provided in Section 3. It can be observed that the material parameter ratios $\lambda^{(1)} = \lambda^{(2)} = 1$, and the longitudinal strain $\varepsilon_A = 0$ in this example. The coefficients of matrix $\mathbf{Q}$ are given by Eq. (11) in terms of the components of matrices $\mathbf{N}^{(k)}$. For the considered problem $\mathbf{Q} = \mathbf{N}^{(2)}$, so that:

$$\mathbf{Q} = \begin{pmatrix} 3.407 & -1.778 \\ -2.407\frac{a^2}{R^2} & 2.778\frac{a^2}{R^2} \end{pmatrix},$$

and matrix $\mathbf{P}$ is of no interest because it is multiplied by $\varepsilon_A = 0$. Now, all integration constants can be found from Eq. (14):

$$A_2 = \frac{1}{3.57 + 0.504\frac{a^2}{R^2}}, \quad B_2 = -\frac{0.706}{3.57\frac{R^2}{a^2} + 0.504},$$

$$A_1 = \frac{0.294}{3.57 + 0.504\frac{a^2}{R^2}}.$$

Fig. 2 shows variation of σ_{rr} and $\sigma_{\theta\theta}$ with radius for several thicknesses of the outer layer. Note that the graphs for $a/R = 0.1$ coincide with the results obtained using Muskhelishvili (1953) formulae for circular inclusion in an infinite plane.

In the case of *in-plane shear*, the solution is given in Section 5. The coefficients of characteristic equation (34) can be calculated as $D_1 = 46.3$, $F_1 = -462.96$, $H_1 = 416.67$, $D_2 = 0.77$, $F_2 = -7.65$, $H_2 = 6.89$. For both layers, the same values $\alpha_{1,2} = \pm 1$, $\alpha_{3,4} = \pm 3$ for the equation roots are obtained. Note that any choice of isotropic material results in these roots of characteristic equation. Distribution of radial and hoop stresses along the line inclined at 45° to x-axis is depicted at Fig. 3. The plots are provided for $a/R \to \infty$; they are indistinguishable from Muskhelishvili (1953) results.

6.2. Remote loading of a cylinder surrounded by an orthotropic interphase layer

In this test problem, we compare our predictions with the results provided in Shokrolahi-Zadeh and Shodja (2008, Example 1, p. 3570). We analyze stress distribution in a core cylinder of radius 1 surrounded by a shell of thickness 0.2 placed in an infinite solid and subjected to a remotely applied combination of tension $2\sigma_0$ in x-direction and compression σ_0 in y-direction. The core and the outside layer (matrix) are transversely isotropic. The shell is cylindrically orthotropic. To evaluate the influence of the shell's anisotropy, we consider three choices for its material parameters. The case considered by Shokrolahi-Zadeh and Shodja (2008) is de-

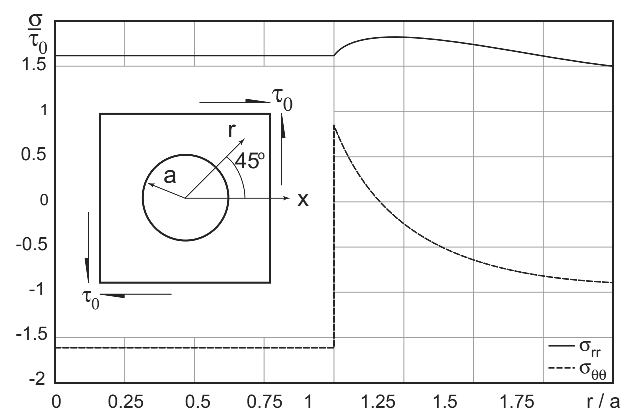

Fig. 3. Distribution of σ_{rr} and $\sigma_{\theta\theta}$ stress components along the line inclined at 45° to x-axis in a composite cylinder with isotropic constituents subjected to transverse shear τ_0.

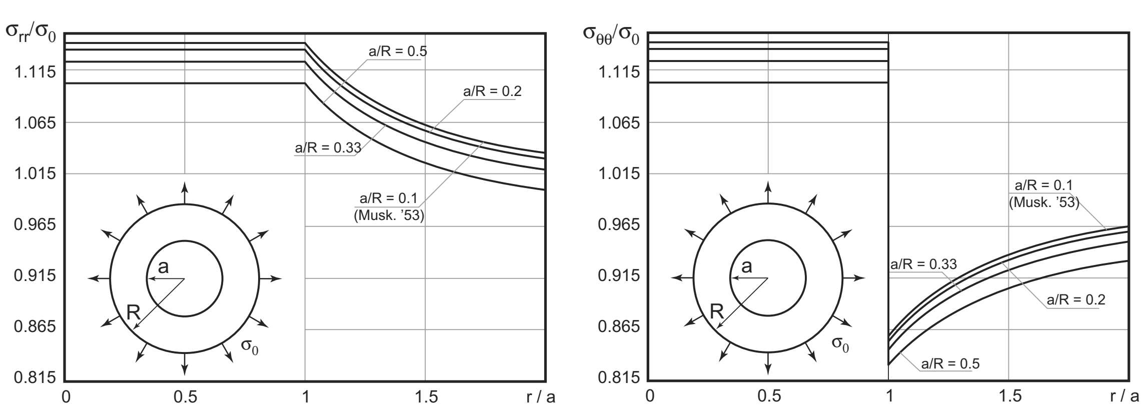

Fig. 2. Stresses in an isotropic fiber surrounded by a layer of isotropic matrix subjected to transverse hydrostatic loading σ_0.

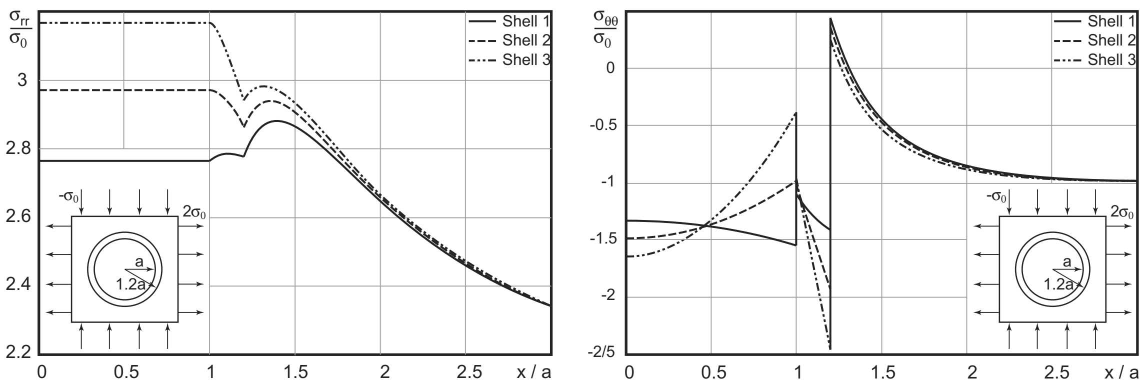

Fig. 4. Distribution of normalized σ_{rr}/σ_0 and $\sigma_{\theta\theta}/\sigma_0$ stress along the x-axis for in-plane biaxial loading.

Table 2
Mechanical properties of constituents in C/C composite.

Layer	R_{i+1} (μm)	C_{rr} (GPa)	$C_{\theta\theta}$ (GPa)	C_{zz} (GPa)	$G_{r\theta}$ (GPa)	$G_{\theta z}$ (GPa)	G_{rz} (GPa)
Fiber	5	15.361	224.987	224.987	9.756	63.082	9.756
2	5.8	25.166	37.189	37.189	22.362	19.004	22.362
3	9.8	23.863	38.496	38.496	22.272	18.466	22.272
4	10.8	24.953	37.300	37.300	22.332	18.911	22.332
5	11.18	24.189	38.096	38.096	22.309	18.609	22.309

noted as "Shell 2". The material properties of constituent materials are given in Table 1.

Fig. 4 presents distribution of radial and hoop stresses along the x-axis. As expected, our results for "Shell 2" model coincide with the solution of Shokrolahi-Zadeh and Shodja (2008). It can also be seen that the increase in the radial stiffness of the shell results in more radial stress transmitted to the inner cylinder, as well as bigger jumps in the hoop stresses.

6.3. Hydrostatic loading of a carbon fiber surrounded by layers of pyrolytic carbon

This example is relevant for carbon/carbon composites (C/C) manufactured by chemical vapor infiltration. The infiltration procedure results in carbon fibers being surrounded by concentric layers of pyrolytic carbon (PyroC) of different texture, see Reznik and Hüttinger (2002) and Piat et al. (2003). The level of texture determines the orthotropy of material stiffness tensor. In particular, one of the carbon/carbon material systems described in Reznik et al. (2003) and Piat et al. (2008) can be treated as a fiber surrounded by four layers of pyrolytic carbon with mechanical properties provided in Table 2. We consider hydrostatic loading of such a material system. Solution of this problem is not only relevant to thermal treatment of carbon/carbon composites but can also be used to predict the composite's overall bulk modulus, see Tsukrov et al. (2009). Fig. 5 presents distributions of the radial and hoop components of stress. Note the significant jump in the hoop stress at the interface between the stiffer fiber and relatively soft pyrolytic carbon. Also, significant anisotropy of constituent materials results in a very pronounced deviation from the homogeneous stress field usually assumed for an isotropic fiber in the isotropic matrix following the famous results of Hardiman (1954) and Eshelby (1957).

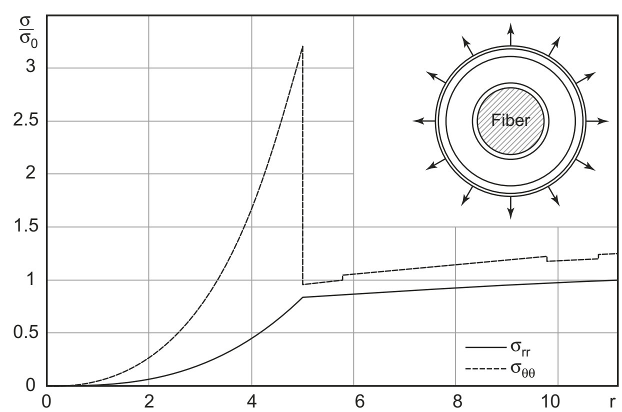

Fig. 5. Radial distribution of normalized σ_{rr}/σ_0 and $\sigma_{\theta\theta}/\sigma_0$ stress components for hydrostatic loading σ_0 of a carbon fiber surrounded by layers of PyroC.

7. Conclusion

This paper presents cylindrically orthotropic elasticity solutions for a laminated cylinder subjected to homogeneous loading applied to its external surface. Explicit expressions for displacement and stress components are given for three loadcases: transverse hydrostatic tension combined with (or considered separately from) axial elongation (Eqs. (6) and (7)), longitudinal shear loading (Eqs. (21), (22) and (24)), and transverse shear (Eq. (36)). All of these expressions contain sets of integration constants having different values for different layers of the cylinder. Due to the assumption of perfect bonding between layers, in all three loading cases the integration constants can be expressed in terms of the core cylinder constants, see Eqs. (12), (26) and (38), respectively. The core cylinder constants are related to the constants of the outer layer (Eqs. (13), (29) and (42)) which are found from the corresponding boundary conditions.

Acknowledgments

The authors gratefully acknowledge the financial support of the National Science Foundation through the Division of Materials Research Grant DMR-0806906"Materials World Network: Multi-

Scale Study of Chemical Vapor Infiltrated Carbon/Carbon Composites" (Program Director for Ceramics Dr. L.D. Madsen). This collaborative international project is also supported by the German Research Foundation (DFG). Florian Termens from the French Institute for Advanced Mechanics (IFMA) participated in the verification of the cylindrically orthotropic solutions as part of his study abroad placement with the University of New Hampshire supervised by Prof. Y. Lapusta.

References

Avery, W.B., Herakovich, C.T., 1986. Effect of fiber anisotropy on thermal stresses in fibrous composites. J. Appl. Mech. 53, 751–756.

Benveniste, Y., Dvorak, G.J., Chen, T., 1991. On effective properties of composites with coated cylindrically orthotropic fibers. Mech. Mater. 12, 289–297.

Chatzigeorgiou, G., Charalambakis, N., Murat, F., 2008. Homogenization problems of a hollow cylinder made of elastic materials with discontinuous properties. Int. J. Solids Struct. 45, 5165–5180.

Chen, T., Dvorak, G.J., Benveniste, Y., 1990. Stress fields in composites reinforced by coated cylindrically orthotropic fibers. Mech. Mater. 9, 17–32.

Christensen, R.M., Lo, K.H., 1979. Solutions for effective shear properties in three phase sphere and cylinder models. J. Mech. Phys. Solids 27, 315–330.

Eshelby, J.D., 1957. The determination of the elastic field of an ellipsoidal inclusion and related problems. Proc. Roy. Soc. Lond. Ser. A 241, 376–396.

Gal, D., Dvorkin, J., 1995. Stresses in anisotropic cylinders. Mech. Res. Commun. 22, 109–113.

Garboczi, E.J., Bentz, D.P., 1997. Analytical formulas for interfacial transition zone properties. Adv. Cement-Based Mater. 6, 99–108.

Hardiman, N.J., 1954. Elliptic elastic inclusion in an infinite elastic plate. Q. J. Mech. Appl. Math. 7, 226–230.

Hashin, Z., 1990. Thermoelastic properties and conductivity of carbon/carbon fiber composites. Mech. Mater. 8, 293–308.

Hashin, Z., 2002. Thin interphase/imperfect interface in elasticity with application to coated fiber composites. J. Mech. Phys. Solids 50, 2509–2537.

Hashin, Z., Rosen, B.W., 1964. The elastic moduli of fiber reinforced materials. J. Appl. Mech. 46, 543.

Hervé, E., Zaoui, A., 1995. Elastic behavior of multiply coated fiber reinforced composites. Int. J. Eng. Sci. 33, 1419–1433.

Honjo, K., 2006. Thermal stresses and effective properties calculated for fiber composites using actual cylindrically-anisotropic properties of interfacial carbon coating. Carbon 45, 865–872.

Kachanov, M., Shafiro, B., Tsukrov, I., 2003. Handbook of Elasticity Solutions. Kluwer Academic Publishers, Dordrecht.

Kanaun, S.K., Kudriavtseva, L.T., 1989. Elastic and thermoelastic characteristics of composites reinforced with unidirectional fibre layers. Appl. Math. Mech. 53, 628–636.

Lutz, M.P., Zimmerman, R.W., 1996. Effect of the interphase zone on the bulk modulus of a particulate composite. J. Appl. Mech. 63, 855–861.

Lutz, M.P., Zimmerman, R.W., 2005. Effect of an inhomogeneous interphase zone on the bulk modulus and conductivity of a particulate composite. Int. J. Solids Struct. 42, 429–437.

Muskhelishvili, N.I., 1953. Some Basic Problems of the Mathematical Theory of Elasticity. Noordhoff, Groningen-Holland.

Piat, R., Reznik, B., Schnack, E., Gerthsen, D., 2003. Modeling the effect of microstructure on the elastic properties of pyrolytic carbon. Carbon 41, 1858–1861.

Piat, R., Tsukrov, I., Böhlke, T., Bronzel, N., Shrinivasa, T., Reznik, B., Gerthsen, D., 2008. Numerical studies of the influence of textural gradients on the local stress concentrations around fibers in carbon/carbon composites. Commun. Numer. Meth. Eng. 24, 2194–2205.

Reznik, B., Hüttinger, K.J., 2002. On the terminology for pyrolytic carbon. Carbon 40, 621–624.

Reznik, B., Gerthsen, D., Zhang, W., Hüttinger, K.J., 2003. Texture changes in the matrix of an infiltrated carbon fiber felt studied by polarized light microscopy and selected area electron diffraction. Carbon 41, 376–380.

Savin, G.N., 1961. Stress Concentrations Around Holes. Pergamon Press, Oxford.

Sevostianov, I., Kachanov, M., 2007. Effect of interphase layers on the overall elastic and conductive properties of matrix composites. Applications to nanosize inclusion. Int. J. Solids Struct. 44, 1304–1315.

Shokrolahi-Zadeh, B., Shodja, H.M., 2008. Spectral equivalent inclusion method: anisotropic cylindrical multi-inhomogeneities. J. Mech. Phys. Solids 56, 3565–3575.

Tarn, J.-Q., Wang, Y.-M., 2001. Laminated composite tubes under extension, torsion, bending, shearing and pressuring: a state space approach. Int. J. Solids Struct. 38, 9053–9075.

Theotokoglou, E.E., Stampouloglou, I.H., 2008. The radially nonhomogeneous elastic axisymmentric problem. Int. J. Solids Struct 45, 6535–6552.

Tsukrov, I., Piat, R., Novak, J., Schnack, E., 2005. Micromechanical modeling of porous carbon/carbon composites. Mech. Adv. Mater. Struct. 12, 43–54.

Tsukrov, I., Drach, B., Gross, T.S., 2009. Influence of anisotropy of pyrolytic carbon on effective properties of carbon/carbon composites. In: Proceedings of the 17th International Conference on Composite Materials – ICCM17, Edinburgh, UK.

Walpole, L.J., 1969. On the overall elastic moduli of composite materials. J. Mech. Phys. Solids 17, 235–251.

Wang, W., Jasiuk, I., 1998. Effective elastic constants of particulate composites with inhomogeneous interphases. J. Compos. Mater. 32, 1391–1424.